Thermochimica Acta, 143 (1989) 265–282
Elsevier Science Publishers B.V., Amsterdam – Printed in The Netherlands

TEMPERATURE-PROGRAMMED CHARACTERIZATION OF SYNTHETIC CALCIUM-DEFICIENT PHOSPHATE APATITES

ANNE MORTIER, JACQUES LEMAITRE* and PAUL G. ROUXHET

Université Catholique de Louvain, Laboratoire de Chimie des Interfaces, Place Croix du Sud 1/5, B-1348 Louvain-la-Neuve (Belgium)

(Received 25 July 1988)

ABSTRACT

Several calcium-deficient hydroxyapatites (DAp) samples were synthesized by aqueous precipitation under controlled conditions, and compared with a commercial hydroxyapatite (HAp) and an equimolar mixture of HAp and dicalcium phosphate (DCP). The samples were analysed using temperature-programmed dehydration (TPR). The results were compared with X-ray diffraction (XRD), and IR spectroscopy data. They show that a variety of calcium phosphate precipitates with Ca/P close to 1.50, ranging from DAp to mere mixture of HAp and DCP, can be obtained according to the synthesis conditions. Typical DAp moieties have two characteristic TPR bands: a wide band in the range 300–680 °C, and a sharper one in the range 700–900 °C. The first band can be assigned to the slow conversion of DAp into a transitory apatite structure partially substituted by hydrogenophosphate and pyrophosphate groups; at higher temperatures, the pyrophosphate groups and the remaining hydrogenophosphate ones will react with the hydroxyl groups of the apatite structure, thereby producing a TPR peak at 700–900 °C. β-Tricalcium phosphate is formed as a result of the latter thermal transformation. Samples containing residual DCP, even in small amounts (> 3%), exhibit a sharp TPR peak in the range 400–600 °C, which can be ascribed to the conversion of DCP into β-calcium pyrophosphate. The high sensitivity of TPR to the presence of DCP allows true DAp to be discriminated from mixtures of calcium phosphates exhibiting the same Ca/P atomic ratio.

INTRODUCTION

The accurate characterization of calcium phosphate apatites either synthesized by precipitation in aqueous solutions, or formed naturally during bone mineralization remains a problem which has still not been completely solved. From a crystallographic point of view, these solids generally present the characteristic X-ray diffraction pattern of hydroxyapatite $Ca_5(OH)(PO_4)_3$

* Author to whom correspondence should be addressed: Ecole Polytechnique Fédérale de Lausanne, Laboratoire de Technologie des Poudres, c/o Bâtiment Chimie, CH-1015 Lausanne-Ecublens, Switzerland.

0040-6031/89/$03.50

(referred to below as HAp), although broadened diffraction lines often point to poorly crystallized specimens. Whereas the Ca/P atomic ratio of HAp is equal to 1.67, it can vary from 1.67 to 1.33 for precipitated apatites. Precipitates having the lowest ratio often present a diffraction line at 18.7 Å [1]. The corresponding compound, octacalcium phosphate (OCP), is best described by the formula $Ca_8H_2(PO_4)_6 \cdot 5H_2O$ [2]. Compounds with compositions intermediate between HAp and OCP are conventionally called calcium-deficient apatites (DAp) [2–7]. Some authors [8–12] have proposed that they be described by the following formula

$$Ca_{10-z}(HPO_4)_z(PO_4)_{6-z}(OH)_{2-z} \cdot nH_2O$$

corresponding to an apatite structure involving Ca defects and substitution of some PO_4^{3-} groups by HPO_4^{2-} ones.

A variety of methods have been used for synthesizing DAps: (i) rapid precipitation of a calcium phosphate gel (amorphous calcium phosphate, ACP) from aqueous solutions of soluble salts of calcium and phosphate, and subsequent ageing of the gel in controlled conditions of pH and temperature [6,8,13,14]; (ii) neutralization of phosphoric acid by lime, or double decomposition, i.e. aqueous precipitation of a soluble phosphate by a neutral, soluble salt of calcium, while maintaining a constant Ca/P ratio [5,15–17]; (iii) controlled hydrolysis of dicalcium phosphates in aqueous suspensions of either DCP or DCPD [18]; and (iv) alkalinization of an acidic, undersaturated solution of calcium and phosphate ions [7]. Improved precipitation methods, involving the control of the pH and the Ca/P ratio of the mother solution throughout the precipitation, have been used more recently [8,19,20]. However, there is still no agreement as to a simple and reproducible method for the preparation of DAps with controlled particle size and Ca/P ratio.

One remarkable property of DAps having a Ca/P ratio equal to 1.50 is their quantitative conversion to β-tricalcium phosphate (β-TCP, also referred to as β-whitlockite in earlier works), after heating for a few hours above 900 °C [4]. The same thermal treatment applied to other DAps would result in the formation of an excess of either HAp or β-calcium pyrophosphate (β-$Ca_2P_2O_7$, β-CPP), depending on the value of Ca/P (> 1.50 or < 1.50) [21]. However, β-TCP is formed upon heating not only DAps, but also mere mixtures of HAp and DCP [22]. Therefore, the phase composition of heat-treated calcium phosphate precipitates is not conclusive as to their nature and degree of deficiency.

Some authors have proposed characterizing the deficiency of DAp samples by measuring their HPO_4^{2-} content [5,6,9,21–24]. The measurement is based on the quantitative estimate of pyrophosphate groups ($P_2O_7^{4-}$) presumably formed upon heating the sample in the temperature range 500–600 °C, as a result of the condensation of HPO_4^{2-} groups in the apatite structure. The determination can be performed either by chemical analysis [6,14] or by quantitative IR spectroscopy [9,21]. However, pyrophosphate

Thermal transformation steps of Ca-deficient apatites

$Ca_{10-z}(HPO_4)_z(PO_4)_{6-z}(OH)_{2-z}\cdot nH_2O$

$<250°C$ (I) ↓

$Ca_{10-z}(HPO_4)_z(PO_4)_{6-z}(OH)_{2-z}\cdot(H_2O)_z+(n-z)H_2O$

250-600°C (II) ↓ (reaction(1))

$Ca_{10-z}(HPO_4)_{2z}(PO_4)_{6-2z}(OH)_2$

250-700°C (III) ↓ (reaction(2))

$Ca_{10-z}(P_2O_7)_z(PO_4)_{6-2z}(OH)_2+zH_2O$

700-800°C (IV) ↓ (reaction(3))

$(1-z)Ca_{10}(PO_4)_6(OH)_2+3zCa_3(PO_4)_2+zH_2O$

Elementary reactions of the phosphate groups

(1) $PO_4^{3-}+H_2O\rightarrow HPO_4^{2-}+OH^-$

(2) $2HPO_4^{2-}\rightarrow P_2O_7^{4-}+H_2O$

(3) $P_2O_7^{4-}+2OH^-\rightarrow 2PO_4^{3-}+H_2O$

Fig. 1. Sketch of the thermal-transformation steps of deficient apatites [24].

groups are not only typical of DAp, but are also produced upon thermal treatment at 400–500°C of DCP and OCP [8,21,22,25]. As a result, the mineralogical characterization of a precipitated apatite on the sole basis of the pyrophosphate content of its pyrolysis product at 600°C is not conclusive, as mixtures of HAp, DCP and/or OCP having the same Ca/P ratio could also produce pyrophosphate groups in the same conditions.

Upon heating DAps exhibit a characteristic thermal reaction scheme, as presented in Fig. 1 [24]. According to this scheme, the thermal analysis of dehydration of DAp samples would enable their degree of deficiency to be estimated. Moreover, depending on the exact nature of the sample (e.g. true DAp or HAp/DCP/OCP mixtures) the HPO_4^{2-} groups are expected to exhibit variable reactivities according to their localization, and consequently to produce characteristic peaks in the thermal dehydration pattern.

Although temperature-programmed dehydration studies [commonly referred to as temperature programmed reaction (TPR) or effluent-gas thermal analysis (EGTA)] of typical calcium phosphates (DCPH, HAp, OCP and ACP) have been performed [26–28], TPR has not been used systematically until now in the characterization of calcium phosphate precipitates and the identification of DAp samples.

In the present study we examined the potential of TPR in characterizing precipitated apatites, and particularly in identifying true DAps from mix-

tures of more-or-less cryptocrystalline HAp and DCP or OCP. For this purpose, the TPR patterns of various apatite samples, synthesized under conditions which were the most likely to produce true DAp, and those of commercial products sold as hydrated TCP or HAp, were analysed and compared with the patterns of reference samples. The results were also compared with those obtained using conventional techniques (X-ray diffraction, IR spectroscopy, chemical analysis). Finally, modifications were made to the accepted thermal reaction scheme of DAps in order to explain the particular features of the TPR patterns of well-crystallized DAps having a Ca/P ratio of 1.50.

MATERIALS AND METHODS

Materials

Various apatites were synthesized by hydrolysis of DCP (UCB p.a.) or DCPD (Merck p.a.), following two different methods: (i) the controlled addition of NaOH using a pH-stat, and (ii) the homogeneous alkalinization of the mother solution by the hydrolysis of urea.

In method (i) the desired amount of the solid reactant was suspended in distilled water, and the initial pH adjusted using HNO_3 or NaOH solutions. The suspension was then placed in a thermostatted bath at the desired temperature (80 or 90 °C) and aged under continuous stirring. The pH of the suspension was maintained at the desired value by the controlled addition of a 0.5-M NaOH solution, using a pH-stat Radiometer ETS822.

In method (ii) the desired amount of solid reactant (10 g l^{-1}) was suspended in distilled water, after adjusting the pH to the desired level using 1-M HNO_3. The desired amount of urea was then added (1.8 g l^{-1}). The suspension (5 l) was placed in a double-jacket, pyrex reactor and stirred continuously at a constant rate (100 rpm). The temperature of the reactor was controlled by a programmable, circulation thermostat (Lauda KP 20 D). The temperature was raised linearly so as to reach the desired value (80 or 90 °C) within 1 h. The pH of the solution increased progressively due to the hydrolysis of urea [29].

Samples of series 10, 20 and 30 were prepared according to method (ii), and samples 50 and 60 were synthesized according to method (i). Some samples (series 40 and 70) were prepared using a variation of method (ii): the starting material was a commercial HAp (UCB) (20 g l^{-1} for series 40 and 34 g l^{-1} for sample 70), and the initial pH of the solution was low enough to allow the complete dissolution of the solid reactant; the amounts of urea were increased accordingly (16 g l^{-1} for series 40 and 34 g l^{-1} for sample 70); sample 70 was aged in an oven without any agitation.

TABLE 1

Preparation conditions of the samples

Sample	Starting material	pH		Temp. (°C)	Time (h)
		Initial	Final		
11	DCPD	4.0	7.0	90	23
12	DCPD	4.0	7.0	90	48
13	DCPD	4.0	7.0	90	71
21	DCPD	4.0		80	22
22	DCPD	4.0		80	47
23	DCPD	4.0	6.5	80	71
24	DCPD	4.0	6.6	80	94
31	DCP	4.0		90	23
32	DCP	4.0		90	47
33	DCP	4.0	6.8	90	71
34	DCP	4.0	6.9	90	95
41	HAp	2.0		90	24
42	HAp	2.0		90	48
43	HAp	2.0		90	72
44	HAp	2.0		90	96
50	DCP	3.9	7.4	90	35
60	DCPD	7.9	7.4	90	26
70	HAp	2.0		80	312

The references of the samples and their conditions of preparation are given in Table 1. No special precautions were taken to eliminate carbonic acid from the solution; nevertheless, the IR spectra of the samples show only negligible amounts of carbonate substitution.

The precipitates were filtered, thoroughly washed with distilled water and freeze dried. The dry samples were stored in a desiccator. The preparation conditions of the individual samples are summarized in Table 1. Besides the synthetic samples, a commercial apatitic sample, sold as hydrated tricalcium phosphate (Merck, pure) was used for comparison.

Reference HAp, β-CPP and β-TCP samples were prepared by calcining at 1000 °C either DCP or HAP or an equimolar mixture of these products, respectively. Details of the preparation of the reference samples have been given previously [22].

Methods

The X-ray diffraction spectra were recorded on a Philips-NORELCO PW 1130 diffractometer using Cu $K\alpha$, Ni-filtered radiation ($\lambda = 0.15418$ nm). The quantitative interpretation of the X-ray diffraction data was made for

the heat-treated samples only, because the intensities of the diffraction peaks of the fresh precipitates were markedly affected by their crystallinity. The mineralogical composition of the samples was estimated by measuring the intensity I of the characteristic peaks of the various phases, at $2\theta = 30.9°$ for β-TCP, $2\theta = 29.1°$ for β-CPP, $2\theta = 31.8°$ for HAp. The calibration curves were established using mixtures of either β-CPP or HAp with β-TCP.

The IR spectra were recorded using KBr pellets in a Beckman IR 12 spectrometer. In order to make the spectra quantitatively useful, each sample (20 mg) and the appropriate amount of KBr (980 mg) were weighed accurately and mixed carefully in an agate mortar; the weight of each pellet was 120 mg. Pieces of cardboard with a rectangular perforation (1 cm^2) were used as pellet holders; the powder was placed in the perforation and pressed between two stainless-steel plates.

The temperature-programmed reaction technique (TPR) was used to follow the thermal dehydration of all the samples. Details of the TPR apparatus and operating conditions have been described previously [22]. The samples (about 130 mg) were heated in a stream of argon (25 ml min^{-1}) with a linear heating program (10 °C min^{-1}). The reactor was of the tubular, flow-through type (inner diameter = 0.10 cm).

The presence of pyrophosphate and metaphosphate in selected samples was investigated using semiquantitative tests. The test for pyrophosphate was taken from Etienne [30]; the threshold limit of this method, as determined from solutions of β-CPP, was found to be 50 ppm of P in the form of pyrophosphate ions, with no interference by orthophosphate species. The test for metaphosphate was taken from Neu [31]; the detection threshold was determined using solutions of Graham's salt and was found to correspond to 50 mg l^{-1} of the salt. Assuming that the Graham's salt was composed exclusively of $(NaPO_3)_n$ (where n is the degree of polymerization of the metaphosphates), this corresponds to 15.2 ppm P in the metaphosphate form.

RESULTS

X-ray diffraction

The X-ray diffraction results are summarized in Table 2. The samples collected after the shortest times in series 10, 20, 30 and 40, consist of mixtures of DCP and apatite, and upon heating at 1000 °C gave mixtures of β-TCP and β-CPP. Increasing the ageing time resulted in a decrease in the DCP content of the samples, which became undetectable by the end of the syntheses, except for series 40. Samples 24, 32, 33 and 34 were pure apatites and were converted into pure β-TCP upon heating at 1000 °C. In contrast, samples 12, 13, 50 and 60, also consisting of pure apatite, left an excess of

TABLE 2

X-ray diffraction results

Sample	I_{DCP} [a] (30.2°)	I_{HAp} [a] (31.8°)	Composition of heated sample [b]	
			β-TCP (wt.%)	Phase in excess
11	12	45	98	HAp
12	0	63	95	HAp
13	0	67	79	HAp
21	50	20	19	β-CPP
22	27	38	50	β-CPP
23	7	55	100	–
24	0	64	100	–
31	19	88	66	β-CPP
32	0	100	100	–
33	0	100	100	–
34	0	100	100	–
41	80	7	Weak	β-CPP
42	43	49	39	β-CPP
43	10	75	58	HAp
44	4	90	24	HAp
50	0	54	65	HAp
60	0	65	64	HAp
70	21	67 [c]	100	–
Merck	17	75	100	–

[a] Fresh samples.
[b] Samples calcined for 1 h at 1000 °C.
[c] OCP was also detected.

HAp upon heating. Sample 70 was a complex mixture of DCP, OCP and HAp; the reference sample from Merck was a mixture of DCP and HAp; both samples were converted into pure β-TCP after thermal treatment.

TABLE 3

Thermal transformations [a] of typical precipitates: X-ray diffraction data

Sample	Temperatures (°C)				
	Ambient	520	720	800	100
33	HAp	HAp	HAp	HAp + β-TCP	β-TCP
60	HAp	HAp	HAp + β-TCP		β-TCP + HAp
70	HAp + DCP + OCP	HAP + CPP			β-TCP

[a] Samples were heated in air for 1 h at the cited temperatures.

The thermal evolution of some representative samples has been studied by X-ray diffraction. The results are summarized in Table 3. It can be seen from Table 3 that only sample 70 exhibited the intermediate formation of β-CPP, while samples 33 and 60 were totally or partially converted from HAp to β-TCP without any detectable intermediate phase.

Temperature-programmed reaction

The TPR patterns of the samples are given in Fig. 2. For the sake of convenience, the peaks are denoted below by Greek letters, according to their temperature range. The various peaks observed for the samples under study are summarized in Table 4 together with their usual assignment. Series 10, 20 and 30 exhibit similar evolution with increasing reaction times. The samples collected after the shortest times exhibited a very intense peak δ which decreases for collection at longer times. This decrease was progressive for series 10, and faster for series 10 and 30. The δ peak was progressively replaced by a very broad band δ'; the latter band was particularly well developed in series 30, being already detected together with the peak δ in sample 31. A small peak ϵ appeared on the patterns, the intensity of which increased as the peak δ decreased. The variation in peak ϵ in series 20 was correlated to an increased formation of β-TCP, as evidenced by the X-ray diffraction result presented above. This confirms the previous assignment of this peak (see Table 4) to the thermal transformation of a deficient apatite into β-TCP.

Series 40 exhibited about the same evolution with time as the series described above. However, the peak ϵ did not appear in any pattern whatsoever, even in that of sample 43 for which the X-ray diffraction results indicated the formation of 58 wt.% β-TCP after thermal treatment. The TPR patterns of samples 50, 60 and 70 were more complex: all these samples exhibited a small, enlarged peak at ca. 300 °C (peak γ); moreover, sample

TABLE 4

Assignment of the TPR peaks

Peak	Temperature range (°C)	Reference	Reaction
α	< 200	[22]	Evolution of adsorbed water
β	200–250	[22]	Evolution of crystallization water
γ	250–350	[21]	$Ca_8H_2(PO_4)_6 \cdot 5H_2O \rightarrow 0.5Ca_{10}(PO_4)_6(OH)_2 + CaHPO_4 + 4H_2O$
		[12]	$Ca_8H_2(PO_4)_6 \cdot 5H_2O \rightarrow Ca_8H_2(PO_4)_6 \cdot 4H_2O$
δ	400–600	[11,12]	$2HPO_4^{2-} \rightarrow P_2O_7^{4-} + H_2O$
		[24,26]	$2CaHPO_4 \rightarrow Ca_2P_2O_7 + H_2O$
ϵ	> 700	[20,21]	$P_2O_7^{4-} + 2OH^- \rightarrow 2PO_4^{3-} + H_2O$

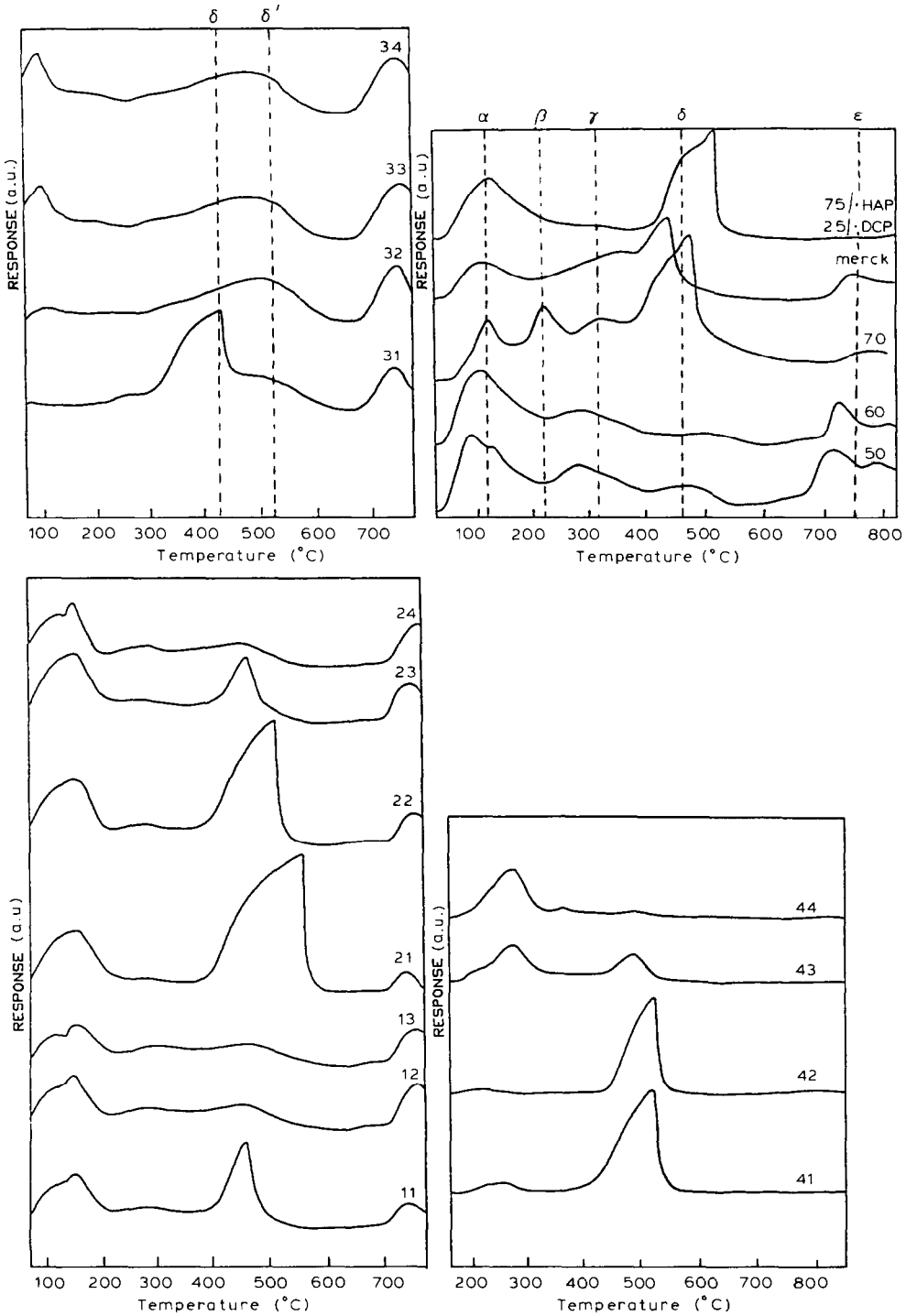

Fig. 2. The TPR patterns of calcium phosphate precipitates.

70 exhibited a medium–large peak at 200 °C (peak β). The assignment of peaks β and γ to OCP, according to the literature, is consistent with the X-ray diffraction data of sample 70. This was not the case for samples 50 and 60, although minor amounts of OCP were possibly present in these samples but below the detection limit of X-ray diffraction. Another feature of samples 50 and 60 was that their peak ϵ was resolved into two peaks, the second one ending slightly below 800 °C. The patterns of the Merck samples and sample 70 were fairly similar, although the low-temperature bands of the former were less well resolved.

The pattern of a DCP/HAp (75/25 wt.%) mixture was taken from ref. 22 and is presented for comparison.

IR spectroscopy

The thermal evolution of the OH^- and $P_2O_7^{4-}$ groups of some representative samples (33, 50, 60, Merck and the HAp-DCP mixture) was investigated

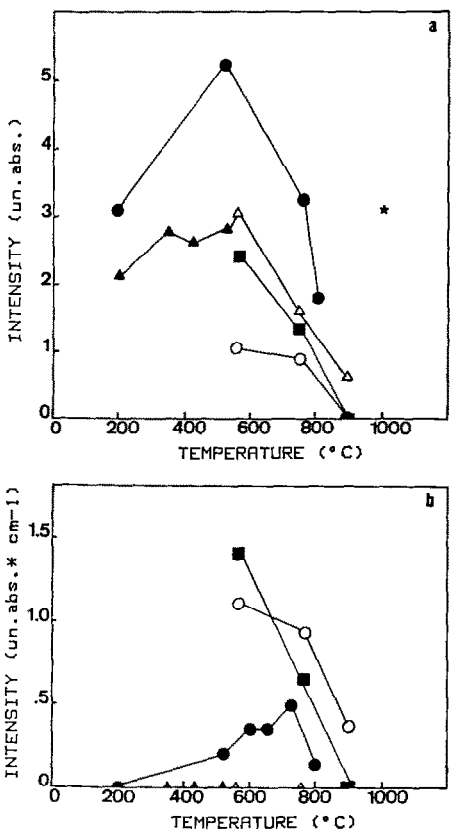

Fig. 3. The variation in the intensities of IR absorption bands versus temperature: (a) OH (3750 cm^{-1}); (b) P_2O_7 (725–755 cm^{-1}). ■, Merck; ○, HAp/DCP (75/25 wt.%); ●, sample 33; △, sample 50; ▲, sample 60.

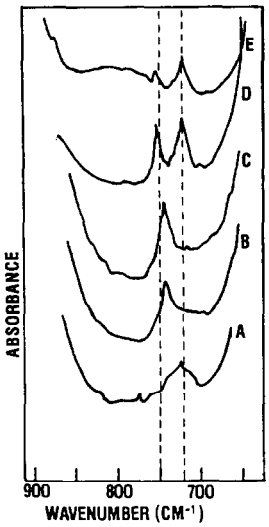

Fig. 4. Evolution of the P_2O_7 IR band (725–755 cm^{-1}) versus temperature. (A) 520 °C; (B) 600 °C; (C) 650 °C; (D) 720 °C; (E) 800 °C. The sample was heated in air for 1 h at the temperatures cited.

using IR spectroscopy. The OH^- groups were monitored using the sharp stretching peak at 3570 cm^{-1} (FWHM = 5 cm^{-1}) [23], which is superimposed on a broad band extending from 3000 to 3700 cm^{-1}. The intensity of this band was estimated from absorbance spectra by reference to a straight baseline drawn between its tails. Figure 3 shows that the OH^- peak intensity reached a maximum at 550 °C for all samples. The increase observed at lower temperatures can be ascribed partly to the removal of the broad band on which the peak is superimposed. However, this does not explain why the OH^- peak of sample 33 became more intense than that of pure HAp, also given in Fig. 3. Such a high intensity agrees with the occurrence of reaction (1) in the reaction pattern presented above (Fig. 1).

The evolution of $P_2O_7^{4-}$ groups was monitored using the characteristic band at 725 cm^{-1} (FWHM = 15 cm^{-1}) [23]. The intensity of this band was estimated by measuring the peak area above the baseline, expressed as absorbance units × cm^{-1}. Figure 3 shows that the intensity of the pyrophosphate band reached a maximum at approximately the same temperature as did the OH^- band, only for the HAp–DCP mixture and for the Merck sample. The band remained below the detection threshold for samples 50 and 60, whatever the temperature of the thermal treatment.

Sample 33 exhibited a particular feature, as shown in Fig. 4. The characteristic pyrophosphate band appeared first at 725 cm^{-1}; as the pretreatment temperature was increased a new, sharper peak appeared at 755 cm^{-1}. After heating to 720 °C, the whole band was resolved into a doublet at 725 and 755 cm^{-1}. The total intensity was maximum near 700 °C, but was

TABLE 5

Results of the semi-quantitative determination of pyrophosphate and metaphosphate species in selected heated samples

Sample	Heat treatment		P(pyro)/P(tot) (%)	P(meta)/P(tot) [a] (%)
	°C	h		
60	560	1	< 5	n.d.
	600	2	< 5	n.d.
33	720	1	5–9	<1.5

[a] n.d., not determined.

always much lower than that of the Merck sample and of the HAp–DCP mixture.

Chemical tests

The results of the chemical tests for selected samples are summarized in Table 5.

DISCUSSION

Characterization of the DAp samples using TPR

Two very different TPR patterns, corresponding to sample 33 and the HAp–DCP mixture, respectively, can be taken as references for the discussion below. As shown previously [22], the HAp–DCP mixture presents the characteristic peaks of apatite (α) and DCP (δ). Besides the α peak, sample 33 exhibits a broad diffuse band ranging from 250 to 600 °C (δ'), instead of the δ peak; a well-defined ϵ peak is also observed at about 750 °C. Although both samples appear to be converted quantitatively into β-TCP at 1000 °C, the X-ray data show that sample 33 consists of pure apatite (see Table 2) and produces no intermediate β-CPP phase whatsoever upon heating (see Table 3). These results contradict the assignment of peak ϵ to the solid–solid reaction of HAp and β-CPP phases, as suggested by Anderson et al. [26], and confirm its assignment to the direct transformation of DAp into β-TCP, as proposed by Monma et al. [24]. Consequently, sample 33 can be considered to be a mineralogically pure apatite having a Ca/P ratio very close to 1.50. Moreover, such a DAp can be easily distinguished from a HAp–DCP mixture by means of its TPR patterns.

From this point on, the joint use of TPR and X-ray data allows the consistent identification of most of the samples studied in this work. Thus, samples 24, 32 and 34 can be considered as pure deficient apatites with Ca/P = 1.50, because they all present the characteristic TPR pattern of

DAp and are converted quantitatively into β-TCP at 1000 °C. Samples 11, 21–23 and 31 are clearly mixtures of DCP and DAp, because their TPR patterns contain both peaks δ and ε, in agreement with the X-ray data reported in Table 2. At high temperatures, these samples are converted into β-TCP and an excess of either HAp or β-CPP, depending on the amount of DCP and on the Ca/P ratio of the DAp present in the fresh precipitate. The formation of HAp from samples 12 and 13 after heating to 1000 °C suggests that they consist in either DAp with Ca/P > 1.50, or in mixtures of DAp with Ca/P = 1.50 and HAp.

Samples in series 40 can be considered as mixtures of HAp and DCP, because their TPR patterns show only the peaks α and δ, and no detectable δ′ or ε peaks. As expected, these samples are converted at 1000 °C into β-TCP admixed with β-CPP or HAp, depending on the amount of DCP present in the fresh precipitate.

Sample 70 is more complex: its TPR pattern includes peaks γ, δ and a weak peak ε, in addition to peaks α and β. This result points to the simultaneous presence of DCP, DAp and/or HAp, and OCP, in agreement with the X-ray data. The fact that sample 70 is quantitatively converted into β-TCP at 1000 °C suggests that enough HAp is present in the sample to bring its Ca/P ratio close to 1.50. The compositions of sample 70 and the Merck sample seem to be fairly similar on the basis of their X-ray and TPR data; however, the presence of OCP in the latter is not detected by X-ray diffraction.

Samples 50 and 60 both present peaks α, γ, δ′ and ε, the latter being resolved into a doublet. The ε doublet together with the presence of peak γ suggest the possible existence in these samples of a OCP-like phase, in such a state of crystallinity that it cannot be detected by X-ray diffraction.

Thermal transformations of DAp and mechanisms of β-TCP formation

The reaction routes leading to the formation of β-TCP will differ according to the mineralogical nature of the precursor: either HAp–DCP mixture or DAp. The case of HAp–DCP mixtures has been discussed in detail previously [22], and so will be considered only briefly here. Both X-ray diffraction and IR spectroscopy results show that β-CPP is formed above 550 °C. Moreover, the OH^- vibration band of the apatite fraction of the samples never reaches a considerable intensity, and its decrease follows closely the DCP to β-CPP transformation; this can be ascribed to the reaction of apatite with the newly formed β-CPP phase. This reaction appears to start at 600 °C and its rate becomes appreciable above 900 °C. β-TCP is thus formed as a result of a solid–solid reaction between β-CPP and HAp.

In the case of DAp, no intermediate β-CPP was detected by X-ray diffraction; therefore the thermal dehydration process probably takes place

in an apatitic framework (Table 3, sample 34). This observation agrees with the reaction scheme of Monma et al. [24] (Fig. 1), according to which reactions (1) and (2) occur simultaneously and are completed by 700 °C. The $P_2O_7^{4-}$ groups, resulting from the condensation of HPO_4^{2-} species in the lattice, would then react with OH^- to form PO_4^{3-} [reaction (3)]. This latter reaction starts at 700 °C and is completed by 800 °C; above 800 °C β-TCP is detected. The IR data obtained for sample 33 agree with the occurrence of reactions (1) and (2), as proposed by Monma et al. [24]. Indeed, the IR spectra show a decrease in both the $P_2O_7^{4-}$ and OH^- species above 500 °C (Fig. 3).

However, in contrast with the assumptions of Monma et al. [24], the quantitative interpretation of the IR data, and the chemical analysis data presented above (Fig. 2 and Table 5) point to a production of pyrophosphate groups which is less than expected. Indeed, were the Ca deficiency of the sample completely compensated for by HPO_4^{2-} in the fresh specimen, and those groups condensating quantitatively into pyrophosphate upon thermal dehydration, about 17% of the P atoms of a typical DAp like sample 33 would belong to pyrophosphate groups, after heating in the range 600–750 °C. However, only 1/3 to 1/2 of this amount is detected by chemical analysis (Table 5), after heating the sample to 720 °C, the temperature at which the maximum pyrophosphate production was shown by the IR data [Fig. 3(b)]. Moreover, the maximum intensity of the pyrophosphate IR peak is effectively 3 times higher for the physical HAp–DCP mixture (Ca/P = 1.50) than for DAp (sample 33).

A good agreement is thus found between chemical analysis and IR results, indicating that the lower intensity of the pyrophosphate IR peak found for DAp samples can be ascribed to a lower concentration of such groups in the intermediate thermal reaction products, rather than to a weakened IR absorbance of pyrophosphate groups enclosed in an apatite structure, as compared to those of a β-CPP phase.

Another interesting feature of the IR spectra of DAp (see Fig. 4) is the shift of the pyrophosphate band from 725 to 755 cm^{-1} when the temperature is raised from 520 to 650 °C, and the appearance of a second peak at 725 cm^{-1} at 720 °C. A similar shift was reported by Monma et al. [24] in the range 600–700 °C, and ascribed to the stabilization of the pyrophosphate groups in an apatite structure. According to Fowler et al. [23], a peak at 755 cm^{-1} appears in the IR spectrum of OCP samples heated directly at 400–600 °C; the normal pyrophosphate peak at 725 cm^{-1}, characteristic of the β-CPP phase, is observed instead for samples heated progressively to 500 °C. However, these authors did not mention any doubling of this peak.

The presence of a doublet at 725 and 755 cm^{-1} in the IR spectra of metaphosphates has been reported by Lecomte et al. [32]. However, the distinct thermal evolution of these two peaks precludes their assignment to a single species such as metaphosphate. Moreover, chemical testing gives no

evidence for any metaphosphate in sample 33, after heating at 720 °C (Table 5). The same conclusion has been reached to by Fowler et al. in the case of OCP [23].

Hence, it is reasonable to dismiss reaction mechanisms involving the intermediate formation of condensed phosphate groups such as cyclic polyphosphates. This result points to the formation of a second pyrophosphate species, appearing at higher temperatures, and distinct from the so-called "stabilized" pyrophosphate groups. As a matter of fact, the latter appear to be less stable than the former, because the IR peak vanishes between 720 and 800 °C, while the newly formed pyrophosphate is still detected at 800 °C. This latter observation points to an incomplete conversion into β-TCP, in agreement with X-ray diffraction data (see Table 3).

As compared with the conversion of HAp–DCP mixtures to β-TCP, the thermal transformation of DAp is characterized by the formation of less intermediate pyrophosphate and by the occurrence of its maximum concentration at higher temperatures. Moreover, the OH^- band intensity is found to decrease in the range 600–720 °C, while the pyrophosphate band intensity continues to increase. This fact cannot be explained in the frame of the reaction scheme proposed by Monma et al. [24], and suggests that the association of steps (III) and (IV) to reactions (2) and (3), respectively (Fig. 1), is not as clear-cut as previously thought. The present results show that more pyrophosphate groups are still formed as a result of reaction (2), while others are already combining with OH^- groups according to reaction (3), and point to a relative stabilization of HPO_4^{2-} with respect to the $P_2O_7^{4-}$ groups in the apatite structure of well-crystallized DAps.

This effect is also apparent from the comparison of the TPR patterns of samples 24 and 33 (Fig. 2). The maximum temperature of band δ' is about 80 °C higher for sample 33, while no marked difference is observed for band ϵ, indicating that reaction step (III) proceeds more slowly in sample 33, while step (IV) is almost unaffected. This effect has been ascribed previously [33] to differences in crystal size (0.25×10.0 μm for sample 33, 0.10×2.0 μm for sample 24).

The above conclusions can be summarized in the following modification of the reaction pattern proposed by Monma et al. [24]

$$Ca_{10-z}(HPO_4)_{2z}(PO_4)_{6-2z}(OH)_2$$

350–720 °C (III) ↓ reactions (2) and (3)

$$Ca_{10-z}(P_2O_7)_{z-s}(PO_4)_{6-2z+2s}(OH)_{2(1-s)} + (z+s)H_2O$$

700–900 °C (IV) ↓ reaction (3)

$$(1-z)Ca_{10}(PO_4)_6(OH)_2 + 3zCa_3(PO_4)_2 + (z-s)H_2O$$

in which reactions (2) and (3) both contribute to step (III). The modified reaction pattern shown above leads us to reconsider the assignment of some

TPR peaks. Reactions (2) and (3) would contribute to peak δ' and lead to the formation of a metastable apatite structure, partially dehydroxylated and substituted by $P_2O_7^{4-}$ groups. Reaction (3) would contribute to peak ϵ, and correspond to the recrystallization of the apatite into β-TCP.

Estimation of the Ca deficiency of DAps by chemical assay of P_2O_7 groups

Some authors have proposed estimating the degree of Ca deficiency of DAps by determining their HPO_4^{2-} content [5,6,9,21–24]. The suggested method consists in making an assay of the pyrophosphate groups presumably formed upon their quantitative thermal condensation upon heating in the range 400–600 °C, using either chemical analysis [6,14] or quantitative IR spectroscopy [9,21]. The results presented above cast doubt on the general validity of this method. Indeed, the results show that quantitative condensation of the hydrogenophosphate groups is not observed in well-defined DAps such as sample 33 after heating up to 720 °C, whereas both hydrogenophosphate and pyrophosphate groups have already begun to react with OH^- groups above 500 °C. Even in the case of HAp–DCP mixtures, the reaction between pyrophosphate and OH^- groups has been detected at temperatures as low as 600 °C. The most appropriate temperature and time of heating to ensure the quantitative conversion of hydrogenophosphate to pyrophosphate in the framework of DAp, if they exist, therefore appear to depend on the nature of the DAp sample under study. Consequently, the experimental conditions of heating found satisfactory for assaying the deficiency of samples prepared under certain conditions (e.g. as in refs. 14 and 21) should be applied with caution to samples prepared using a different method.

CONCLUSIONS

TPR is a sensitive technique allowing the characterization of calcium phosphate precipitates, the complexity of which is not always evidenced by X-ray diffraction. TPR makes clear the difference between DAp and HAp or HAp–DCP mixtures, and allows "true" DAp with Ca/P = 1.50 to be discriminated from complex mixtures which convert quantitatively into β-TCP upon heat treatment.

The combined use of TPR and X-ray diffraction has shown that a variety of synthetic calcium phosphate precipitates, ranging from DAp to mere mixtures of HAp and DCP, could be used as precursors of β-TCP. Depending on the precursor, various thermal reactions can lead to the formation of β-TCP. IR spectroscopy and chemical analysis have shown that the hydrogenophosphate to pyrophosphate conversion was not necessarily a quantitative process during the thermal conversion of DAp to β-TCP.

ACKNOWLEDGEMENTS

The authors thank A. Kaddoury and J. Rocq for experimental assistance in the synthesis of the samples. They acknowledge the support of Dr. E. Munting and of the Laboratory of Orthopaedic Surgery (Catholic University of Louvain, Brussels, Belgium). The financial support of the "Service de la Programmation de la Politique Scientifique" (Concerted Action Physical Chemistry of Interfaces and Biotechnology, Programme PREST) is also gratefully acknowledged.

REFERENCES

1 ASTM Powder Diffraction File, card no. 26-1056A.
2 W.E. Brown, J.P. Smith, J.R. Lehr and A.W. Frazier, Crystallographic and Chemical Relations between Octacalcium Phosphate and Hydroxyapatite, Nature, 196 (1962) 1050.
3 A.S. Posner and A.M. Perloff, Apatite Deficient in Divalent Cations, J. Res. Nat. Bur. Stand., Sect. A, (1957) 279–285.
4 J. Benard, Combinaisons avec le phosphore, in P. Pascal (Ed.), Nouveau traité de Chimie Minérale, Tome IV, Le Calcium, Masson, Paris, (1958) p. 455.
5 L. Winand, Etude physico-chimique du phosphate tricalcique hydraté et de l'hydroxyl-apatite, Ann. Chim., 16 (1961) 941–967.
6 J.C. Heughebaert and G. Montel, Sur l'existence d'une série de solides de composition variable, correspondant au phosphate tricalcique précipité, C. R. Acad. Sci., Ser. C, 270 (1970) 1585–1588.
7 J.L. Meyer and E.D. Eanes, A Thermodynamic Analysis of the Secondary Transition in the Spontaneous Precipitation of Calcium Phosphate, Calcif. Tissue Res., 25 (1978) 209–216.
8 N.C. Blumenthal, F. Betts and A.S. Posner, Calcif. Tissue Int., 33 (1981) 111.
9 S.J. Joris and C.H. Amberg, J. Phys. Chem., 75 (1971) 3167.
10 S.J. Joris and C.H. Amberg, J. Phys. Chem., 75 (1971) 3172.
11 E.E. Berry, J. Inorg. Nucl. Chem., 29 (1967) 317.
12 E.E. Berry, J. Inorg. Nucl. Chem., 29 (1967) 1585.
13 R. Wallaeys, Ann. Chem., Ser. 12, 7 (1952) 808.
14 J.C. Heughebaert, Thesis, Institut National Polytechnique de Toulouse, 1977.
15 E.C. Moreno, T.M. Gregory and W.E. Brown, J. Res. Nat. Bur. Stand. (U.S.), 72A (1968) 773.
16 B. Tomazic and G.H. Nancollas, J. Coll. Interface Sci., 50 (1975) 451.
17 S. Shimbayashi, T. Aoyama and M. Nakagaki, Chem. Pharm. Bull., 30 (1982) 3872.
18 G. Montel, Bull. Soc. Chim. Fr., (1953) 506.
19 J.F. de Rooij, J.C. Heughebaert and G.H. Nancollas, J. Coll. Interface Sci., 100 (1984) 350.
20 T.P. Feenstra and P.L. de Bruyn, J. Phys. Chem., 83 (1979) 475.
21 A. Gee and V.R. Deitz, J. Am. Chem. Soc., 77 (1955) 2961.
22 A. Mortier, J. Lemaitre and P. Rouxhet, Thermochim. Acta, 113 (1987) 133.
23 B.O. Fowler, E.C. Moreno and W.E. Brown, Arch. Oral Biol., 11 (1966) 477.
24 H. Monma, S. Ueno and T. Kanazawa, J. Chem. Technol. Biotechnol., 31 (1981) 15.
25 N.W. Wikholm, R.A. Beebe and J.S. Kittelberger, J. Phys. Chem., 79 (1975) 853.
26 C.W. Anderson, R.A. Beebe and J.S. Kittelberger, J. Phys. Chem., 78 (1974) 1631.

27 H. Furedi-Milhofer, V. Hlady, F.S. Baker, R.A. Beebe, N.W. Wikholm and J.S. Kittelberger, J. Colloid Interface Sci., 70 (1979) 1.
28 J.M. Sedlak and R.A. Beebe, J. Colloid Interface Sci., 47 (1974) 483.
29 J.A. Parodi, R.L. Hickok, W.G. Segelken and J.R. Cooper, J. Electrochem. Soc., 112 (1965) 688.
30 H. Etienne, Ind. Chim. Belge, 28 (1953) 340.
31 R. Neu, Z. Anal. Chem., 31 (1950) 102.
32 J. Lecomte, A. Boulle and M. Domine-Berges, Mem. Soc. Chim. (Paris), (1948) 764.
33 A. Mortier, J. Lemaitre, L. Rodrique and P.G. Rouxhet, J. Solid State Chem., in press.